SMGroup

# Quantitative Evaluation of Anterior and Posterior Segment Parameters in Glaucoma Using Optical Coherence Tomography

**Xiaogang Wang[1] and Jing Dong[2]**

[1]Shanxi Eye Hospital, PR China

[2]The First Hospital of Shanxi Medical University, PR China

***Corresponding author:** Xiaogang Wang, Shanxi Eye Hospital, Shanxi, PR China, Email: 13834246830@163.com

**Published Date:** October 30, 2015

## INTRODUCTION

Glaucoma, as the second leading cause of blindness worldwide, irreversibly damages patients' structural and functional tissues, such as the filtration angle, Retinal Ganglion Cell Complex **(GCC)**, Retinal Nerve Fiber Layer Thickness **(RNFL)**, Choroidal Thickness **(CT)** and optic nerve head microcirculation [1,2].

Limited resources of histological samples, especially for the early stages of glaucoma, have impeded a better understanding of early anatomical changes in glaucoma. Using different imaging technologies enabled the objective and quantitative assessment of structural damages in several ocular diseases. Optical coherence tomography **(OCT)**, introduced as noninvasive imaging technology in the early 1990s, is commonly used in ophthalmic clinics for the diagnosis and management of glaucoma [3].

## COMMERCIALLY AVAILABLE OCT TECHNOLOGY

OCT is based on the principle of low-coherence interferometry, which detects the time of flight delay of light reflected from the ocular tissues [4]. OCT is analogous to ultrasound; however, OCT detects reflections of infrared light waves from different ocular structure rather than acoustic waves. There are primarily two prototypes for OCT technology in the clinical setting: the Time-Domain **(TD)**-OCT and the Spectral-Domain **(SD)**-OCT [5]. TD-OCT uses low-coherence light, which will be split into two beams at a partially reflecting mirror. One beam is focused on the

tissue of interest, whereas the other beam is directed at a mirror, which is attached to a moving reference arm. The two beams recombine at a specific photo detector. Then, the interference is assigned to evaluate the intensity of the back reflected light, which corresponds to the structural tissue. SD-OCT evaluates the intensity of the back reflected light without moving the reference arm, considerably saving scanning time. SD-OCT encodes the time delay at each depth by using the Fourier transform of the interference spectrum of the light signals. Moreover, SD-OCT uses a broader wavelength to improve the image resolution. Based on those combinations, SD-OCT can acquire more data with better resolution images at higher scanning speed than TD-OCT, which makes it a valuable tool for retinal disease evaluation [6,7].

With higher axial resolution, faster scanning speed and lower susceptibility to eye movement artifacts, the SD-OCT offers more detailed, structural information and improved repeatability and reproducibility than TD-OCT. However, several studies have demonstrated that they have statistically similar diagnostic accuracy in several glaucoma diagnostic parameters [8,9].

## ANTERIOR SEGMENT AND POSTERIOR SEGMENT OCT DEVICES

Based on different light sources, the Anterior-Segment **(AS)**-OCT devices can be categorized into two systems: dedicated systems using 1310 nm (Zeiss Visante AS-OCT, Tomey CASIA, Heidelberg SL-OCT, etc.) and systems converted from the regular retinal scanner using 830 nm (Optovue Avanti RTvue XR, Optovue RTvue, Optovue iVue, Zeiss Cirrus, Heidelberg Spectralis, etc) [10]. Because of the differences in light sources, there are several functional differences between the two systems. A longer wavelength (1310 nm) dedicated system can provide full view of the anterior chamber, deeper penetration and a small amount of the light can reache the retina due to its strong absorption in the ocular media (Figure 1A). On the contrary, a shorter wavelength (830 nm) system can demonstrate a higher axial resolution but not full view of the anterior chamber and limited imaging depth (Figure 1B).

For the posterior segment OCT devices, there are two systems: regular systems approximately 830 nm (Optovue Avanti RTvue XR, Optovue RTvue, Optovue iVue, Zeiss Cirrus, Topcon 3D-1000/2000, Heidelberg Spectralis, etc.) and systems using 1050 nm swept laser (Topcon DRI OCT). Several of these retinal OCT devices can provide not only the retinal structural information (e.g., macular thickness, RNFL, CT, and lamina cribrosa depth etc) but also the retinal microcirculation information (e.g., Flow Index **(FI)**, blood flow velocity, and vessel density).

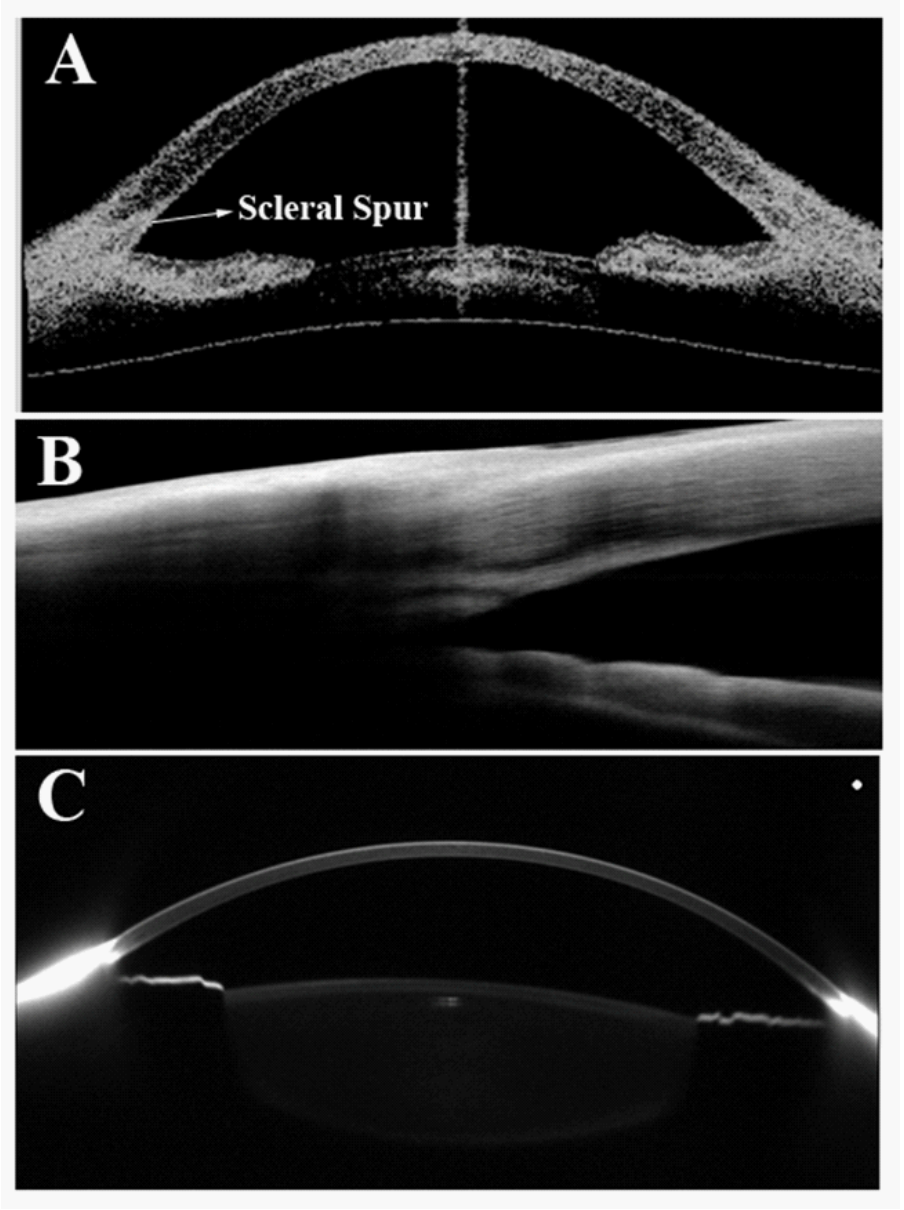


**Figure 1:** Anterior chamber angle cross-sectional images of Time-Domain **(TD)** Anterior Segment Optical Coherence Tomography **(AS-OCT)**, Spectral Domain **(SD)** OCT and Pentacam Scheimpflug system. The scleral spur is visible in the TD AS-OCT (A) Images but not resolvable in the SD AS-OCT (B) and Pentacam Scheimpflug (C) images.

## ANTERIOR SEGMENT PARAMETERS

Gonioscopy, which is considered to be a gold-standard method for measuring the Anterior Chamber Angle **(ACA)**, can provide static and dynamic ACA information. Using this technique,

the ACA width is graded by evaluating the distance between the trabecular meshwork and the iris root. As a contact and subjective examination method, gonioscopy requires an experienced operation technique because of its poor repeatability and reproducibility [11]. Therefore, an easier quantitative and objective method for measuring the ACA could make the results much easier to compare. Cross-sectional imaging technologies, such as ultrasound biomicroscopy, Scheimpflug photography, and OCT, have been used for the quantitative measurement of ACA in a clinical setting.

Compared to gonioscopy, the UBM provides high resolution images (50-$\mu$m lateral and axial resolution in the commercial system) of the ACA and has demonstrated more details regarding ACA since the 1990s. Moreover, UBM, which has a 5-mm depth penetration in the tissue and has the ability to image through opaque media, can demonstrate information regarding the ciliary sulcus and posterior border of the ciliary body because of the higher tissue penetration feature of the acoustic wave. However, UBM has several limitations in the clinical setting, such as requiring contact with the globe, as well as being time-consuming and technician-dependent. More importantly, the inadvertent pressure on the eye cup could influence the anterior chamber configuration [12].

The Scheimpflug imaging technology has been used for quantitatively measuring ACA in the clinical setting. However, the actual ACA recess is hardly visualized due to the poor penetration and light scattering from the sclera and sclera spur (Figure 1C). Therefore, the important structural landmark information in this region can be easily missed.

AS-OCT, which is a non-contact, non-invasive imaging modality can be performed easily and can demonstrate good repeatability and reproducibility in the clinical setting [13]. It demonstrates higher image resolution than UBM, and the noncontact feature of AS-OCT not only gives patients feeling of safety and comfort with respect to its operational but also eliminates any imaging distortion of the ACA and improves the reliability of angle parameter measurements. There are several parameters for ACA evaluation, such as Angle Opening Distance (**AOD** 500 $\mu$m and 750 $\mu$m), Angle Recess Area **(ARA)**, Trabecular-Iris Space Area **(TISA)** and ACA.

AOD: This parameter was first described by Pavlin et al. using UBM [14]. It is the distance from the iris to the angle wall along a perpendicular line to the trabecular meshwork and cornea at two specific distances (500 $\mu$m and 750 $\mu$m) from the scleral spur.

ARA: This parameter was first reported by Ishikawa et al. using UBM [15]. It is the triangular area with three boundaries: 1) Anterior boundary, the AOD 500 $\mu$m or AOD 750 $\mu$m; the apex, the angle recess; 2) Superior boundary, the inner corneoscleral wall and 3) Inferior boundary, the iris surface. Compared to the AOD, the ARA is a theoretically better parameter because it considers the entire contour of the iris surface, not just a single point on the iris. However, the ARA may not be sensitive enough to determine a narrow angle for eyes with deeper angle recess.

TISA: This parameter was reported by Radhakrishnan et al. [16]. It is defined as the trapezoidal area with four boundaries: the superior boundary, the inner corneoscleral wall; the anterior boundary, a perpendicular line from the iris surface to the inner corneoscleral wall at 500 $\mu$m or 750 $\mu$m anterior to the scleral spur; the inferior boundary, the iris surface; and the posterior boundary, a perpendicular line from the scleral spur to the inner corneoscleral wall. Because of the exclusion of the nonfiltering area behind the sclera spur, TISA may better define the actual filtering region. (Figure 2)

ACA: This parameter was first reported by Pavlin et al [14]. Traditionally, it consists of one apex (angle recess) and two arms (drawing lines through the endpoints of AOD 500 $\mu$m). Several researchers have suggested using sclera spur, which is clearer than the angle recess in OCT imaging, as the fulcrum of angle measurement.

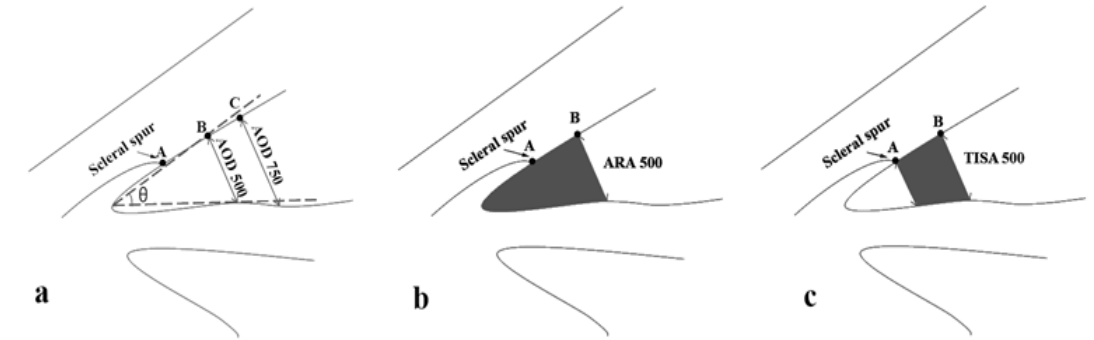


**Figure 2:** Schematic diagram of anterior chamber angle parameters, such as angle opening distance (AOD 500/750), anterior chamber angle (θ), angle recess area (ARA 500), trabecular iris space area (TISA 500), analyzed by ultrasound biomicroscopy and anterior segment optical coherence tomography software. AOD is a distance from the iris to the angle wall along a perpendicular line to the trabecular meshwork and cornea at two specific distances (500 $\mu$m and 750 $\mu$m) from the scleral spur. ACA consists of one apex (angle recess) and two arms (drawing lines through the endpoints of AOD 500). ARA is the triangular area with three boundaries: 1) Anterior boundary, the AOD 500 or AOD 750; the apex, the angle recess. 2) Superior boundary, the inner corneoscleral wall and 3) Inferior boundary, the iris surface. TISA is defined as the trapezoidal area with four boundaries: 1) Superior boundary, the inner corneoscleral wall; 2) Anterior boundary, a perpendicular line from the iris surface to the inner corneoscleral wall at 500 $\mu$m or 750 $\mu$m anterior to the scleral spur; 3) Inferior boundary, the iris surface; and 4) Posterior boundary, a perpendicular line from the scleral spur to the inner corneoscleral wall. Note: Dot A represents the sclera spur. The distance from dot A to dot B and from dot A to dot C is 500 $\mu$m and 750 $\mu$m, respectively.

The quantitative evaluation of the ACA has been studied by many authors. In the study by Radhakrishnan et al., the AOD 500 $\mu$m, ARA 500/750 $\mu$m and TISA 500/750 $\mu$m showed excellent

discriminative ability (the area under the receiver operating characteristic curve ranging from 0.96 to 0.98) to distinguish the narrow angle [16]. Another study also showed that the ACA and AOD 500 parameters demonstrated approximately 90% high sensitivity and specificity to detect an occludable angle [17]. AS-OCT can be not only a useful tool for screening narrow angle but can also quantitatively measure the anterior chamber changes in illumination and Laser Peripheral Iridotomy **(LPI)** situations [18-22]. For those parameters, previous research has demonstrated that AOD 750 is the most significantly useful angle assessment tool for distinguishing a narrow angle using AS-OCT images [23]. Moreover, AS-OCT can be used to evaluate the correlation of the filtering blebs morphology and post-operative IOP control [24-26]. The 3D AS-OCT imaging modality can show more detailed information regarding the internal morphology of filtering blebs and demonstrate the accurate position of the filtration opening on the sclera flap margin after trabeculectomy [27]. Recently, Kojima et al., using 3D AS-OCT found that the filtration opening width at the early stage of post-trabeculectomy may be a prognostic factor for long-term IOP control [28].

There are several limitations of AS-OCT that should be recognized in clinical application. First, several previous reporters found that AS-OCT tended to detect more closed angles than gonioscopy and that this discrepancy may, in part, be attributed to different definitions of angle closure and potential illumination-induced widening of ACA using gonioscopy [29,30]. Second, the sensitivity and specificity of single quantitative AS-OCT parameters are not sufficient enough to perform the population-based screening for closed angle [31,32]. Third, time-domain AS-OCT only captures one or two cross-sectional images at a single scanning, which is not sufficient enough to evaluate the entire ACA and some important information may be missed. It is time-consuming and impractical to obtain 360°ACA information by using the scanning meridian by meridian. Finally, the scleral spur, which is hardly visible in 30% of the OCT scanning images, is an important landmark to realize angle quantitative analysis [23,33]. Moreover, scleral spur identification could also be affected by the juxtaposition of the highly reflective tissues in narrow angles.

## POSTERIOR SEGMENT PARAMETERS

Standard Automated Perimetry **(SAP)** has commonly been regarded as the gold standard method for assessing of progressive damage in glaucoma patients; however, the Visual Field **(VF)** testing demonstrated poor repeatability and substantial variability in several patients [34-36]. OCT can provide noncontact, real-time, and high-resolution cross-sectional retinal structural (RNFL thickness, macular thickness, CT, GCC, LC depth, etc.) and functional images (total retinal blood flow, FI, and vessel density) *in vivo* [8,37-41]. Retinal nerve fiber is derived from the retinal ganglion cell axons. The circumpapillary RNFL thickness will typically change in glaucoma progression. Previous clinical research with large sample sizes have demonstrated that progressive RNFL and structural optic nerve damage could be observed before the detectable

losses on SAP [42-45]. Miki et al. showed that the RNFL loss rate measured using SD-OCT may be a useful tool for identifying patients with high risk of developing VF loss; for the glaucoma suspect eyes, the rate of global RNFL loss was more than twice as fast in eyes that developed VF defects compared with those that did not develop VF defects [46]. However, Hood et al. demonstrated that the en face OCT images based on the average reflectance intensity were better than the traditional OCT RNFL thickness analysis for identifying the details of local glaucomatous damage [47].

The loss of retinal ganglion cells is regarded as a vital step in the pathogenesis leading to thinning RNFL and ONH changing. Ng et al. demonstrated the good repeatability of measuring mascular and perimacular Ganglion Cell Complex **(GCC)** using SD-OCT in 92 non glaucomatous eyes [48]. Recent researches confirmed that the macular GCC can be a useful structure-function indicator in detecting early glaucoma and that it has a strong correlation with frequency-doubling technology perimetry sensitivity and SAP sensitivity [49,50].

The Lamina Cribrosa **(LC)**, a mesh-like structure surrounding and supporting the retinal ganglion cell axons, has been proven to be connected with glaucomatous optic disc and VF changes in human eyes *in vivo* using the Enhanced Depth Imaging OCT **(EDI-OCT)** [38,51-54]. Moreover, elevated Intraocular Pressure **(IOP)** could result in the posterior LC displacement and IOP lowering treatment can reverse this displacement [55-57]. A recent study showed that a reliable time course of anteroposterior LC position and LC depth monitoring could be most useful for early glaucoma treatment through the preperimetric and mild-to-moderate stages [58].

Increased IOP in glaucoma may damage the microcirculation and vascular perfusion around the Optic Nerve Head **(ONH)**. Earlier histological research showed thinner choroid in glaucoma eyes compared to normal eyes, which may support some connection between choroidal morphology changes and glaucoma [59-61]. As the modified version of SD-OCT, the EDI-OCT can likely obtain the full choroidal images *in vivo* [62]. Unfortunately, the majority of the studies regarding CT in glaucomatous eyes scarcely found significant differences in CT both under the fovea and around the ONH compared with healthy controls [63]. Additionally, no significant correlation was found between glaucomatous eyes and the marked thinning or thickening of the choroid in the foveal and parafoveal region [64-66]. However, the difficult clearly discerning characteristic of the choroidal-scleral boundary and the manual segmentation of CT makes the results more variable [67,68].

In addition to the structural changes in glaucoma, previous research has demonstrated that vascular dysfunction may be associated with glaucoma [69-73]. Different methods have been used to detect ocular blood perfusion in clinical practice and experimental research. Prolonged arteriovenous passage times, fluorescein-filling defects in the disc and focal sector hypoperfusion of ONH have been demonstrated in patients with ocular hypertension, primary open-angle glaucoma, low-tension glaucoma and chronic simple glaucoma using Fluorescein Angiography **(FA)** [74-78]. FA and indocyanine green angiography provide qualitative evaluations of retinal and

choroidal circulation although they do not provide objective quantitative measurements. Unlike FA, Laser Doppler Flowmetry **(LDF)** and Laser Speckle Flowgraphy **(LSFG)** can noninvasively measure disc perfusion in glaucoma. Compared to normal subjects, the decreased blood flow in ONH of glaucoma suspects and glaucoma using the single-point LDF has been reported by Hamard et al. and Piltz-Seymour et al. [79,80]. Significantly decreased neuroretinal rim blood flow and peripapillary retinal blood flow were demonstrated in patients with glaucoma using the scanning LDF [81]. Regarding the significantly lower blood flow in ONH of open-angle glaucoma patients, Hafez et al. and Michelson et al. suggested that reduced ONH blood perfusion may manifest earlier than the VF defections [82,83]. Using LSFG, previous research reported lower mean blur rates of ONH and less perfusion at the superior and inferior sectors of disc rim in patients with glaucoma [84,85]. However, the intra-visit repeatability and inter-visit reproducibility of LDF and LSFG are too variable to be used in the clinical diagnosis [86,87]. As a noninvasive imaging technology, using Doppler OCT enable us to obtain precise measurements of total retinal blood flow calculated from the Doppler frequency shift of backscattered light [88]. Using Doppler OCT, previous studies demonstrated not only reduced retinal blood flow in glaucomatous eyes but also the close link among reduced retinal blood flow, thinning retinal neural structure and VF loss [89,90]. Recently, Tan et al. confirmed that the reduced total retinal blood flow for glaucomatous participants compared to healthy controls using the en face Doppler OCT with intra-visit repeatability was approximately 8% for both groups [91]. Although appropriate for large vessels around ONH, Doppler OCT is not sensitive enough to accurately measure the low velocities of small vessels [37].

As an emerging method for measuring local circulation using high-speed OCT, the OCT angiography of ONH or macular area can be quantified using the Split-Spectrum Amplitude-Decorrelation Angiography **(SSADA)** algorithm as FI, and the FI already showed higher intra visit repeatability and intervisit reproducibility (Figure 3) [39,40]. FI was defined as the average decorrelation value within any interesting retinal area, such as ONH, and parafoveal area. Due to the non-linear relationship between decorrelation and flow velocity, the FI primarily measured the area of the large vessels and the area (or vessel density) and velocity of the capillaries [39]. Yali et al. found that the microvascular network was visibly attenuated and that the disc FI was significantly reduced in approximately 25% in patients with glaucoma compared with normal group [71]. Recently, Liu et al. reported that peripapillary FI and prepapillary vessel density in glaucoma were significantly lower than those in healthy control eyes with high repeatability and reproducibility and that these indices were highly correlated with the VF pattern standard deviation in glaucomatous eyes [92].

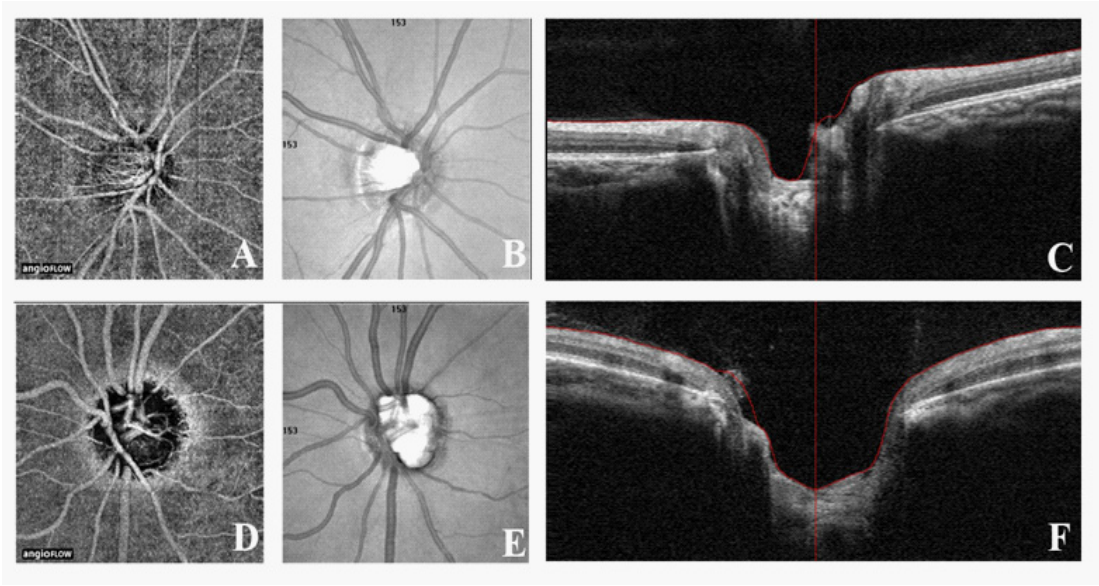


**Figure 3:** Whole depth Optical Coherence Tomography **(OCT)** angiograms (A, D, and en face Maximum projection), en face OCT reflectance (B and E), cross-sectional OCT reflectance (C and F) Of Optic Nerve Head **(ONH)** in the right eye of a normal eye (panels A, B, and C) and the left eye of a perimetric glaucomatous eye (panels D, E, and F). A dense micro vascular network was visible on the OCT angiogram of the normal ONH (A). This micro vascular network was considerably attenuated in the glaucomatous ONH (D). A larger cup/disc ratio was visible on the en face OCT reflectance of the glaucomatous eye (E) than that of the normal eye (B). A larger, deeper cupping of the ONH was demonstrated on the cross-sectional OCT reflectance of the glaucomatous eye (F) than that of the normal eye (C).

## CONCLUSIONS

Commercial time-domain AS-OCT allows noncontact cross-sectional visualization of the anterior chamber and ACA for the first time. Using internal ACA-related software, AS-OCT can quickly evaluate potential blockage of the filtration angle. Moreover, previous studies have shown that many OCT angle parameters, such as AOD 500/750, ARA 500/750, and TISA 500/750, demonstrated good reproducibility and that they all correlated well with gonioscopy in the assessment of closed angles.

High-speed posterior segment OCT allows non-invasive visualization and quantification of both structural and functional information of the retina. Quantitatively, the structural parameters (RNFL thickness, macular thickness, CT, GCC, LC depth and displacement) and functional parameters (total retinal blood flow, FI, and vessel density) can realize vital assessment of the retina for glaucomatous damage, especially for the clinical follow-up post-operation/medicine.

Our preliminary studies and other studies have demonstrated that the majority of these parameters were highly repeatable and reproducible. Moreover, most of them correlated well with VF defects in the detection of glaucomatous damage.

The commercial availability of high-speed anterior and posterior segment OCT systems will allow more ophthalmologists to manage patients and perform research using this new imaging technology. The reliable, quantitative, angle measurements and retinal parameters might eventually allow clinicians to precisely evaluate the risk of acute and chronic glaucomatous damage and better manage these diseases that might potentially cause blindness.

## ACKNOWLEDGEMETS

This work was supported by the National Natural Science Foundation of China under Grant No. 81501544.

### References

1. Mantravadi AV, Vadhar N. Glaucoma. Prim Care. 2015; 42: 437-449.
2. Quigley HA, Broman AT. The number of people with glaucoma worldwide in 2010 and 2020. Br J Ophthalmol. 2006; 90: 262-267.
3. Huang D, Swanson EA, Lin CP, Schuman JS, Stinson WG. Optical coherence tomography. Science. 1991; 254: 1178-1181.
4. Baumal CR. Clinical applications of optical coherence tomography. Curr Opin Ophthalmol. 1999; 10: 182-188.
5. Leitgeb R, Hitzenberger C, Fercher A. Performance of fourier domain vs. time domain optical coherence tomography. Opt Express. 2003; 11: 889-894.
6. Schuman JS. Spectral domain optical coherence tomography for glaucoma (an AOS thesis). Trans Am Ophthalmol Soc. 2008; 106: 426-458.
7. Wojtkowski M, Srinivasan V, Fujimoto JG, Ko T, Schuman JS. Three-dimensional retinal imaging with high-speed ultrahigh-resolution optical coherence tomography. Ophthalmology. 2005; 112: 1734-1746.
8. Wong JJ, Chen TC, Shen LQ, Pasquale LR. Macular imaging for glaucoma using spectral-domain optical coherence tomography: a review. Semin Ophthalmol. 2012; 27: 160-166.
9. Mansouri K, Leite MT, Medeiros FA, Leung CK, Weinreb RN. Assessment of rates of structural change in glaucoma using imaging technologies. Eye (Lond). 2011; 25: 269-277.
10. Huang D, Li Y, Radhakrishnan S. Optical coherence tomography of the anterior segment of the eye. Ophthalmol Clin North Am. 2004; 17: 1-6.
11. Alward WL. A history of gonioscopy. Optom Vis Sci. 2011; 88: 29-35.
12. Pavlin CJ, Harasiewicz K, Sherar MD, Foster FS. Clinical use of ultrasound biomicroscopy. Ophthalmology. 1991; 98: 287-295.
13. Li H, Leung CK, Cheung CY, Wong L, Pang CP. Repeatability and reproducibility of anterior chamber angle measurement with anterior segment optical coherence tomography. Br J Ophthalmol. 2007; 91: 1490-1492.
14. Pavlin CJ, Harasiewicz K, Foster FS. Ultrasound biomicroscopy of anterior segment structures in normal and glaucomatous eyes. Am J Ophthalmol. 1992; 113: 381-389.
15. Ishikawa H, Liebmann JM, Ritch R. Quantitative assessment of the anterior segment using ultrasound biomicroscopy. Curr Opin Ophthalmol. 2000; 11: 133-139.
16. Radhakrishnan S, Goldsmith J, Huang D, Westphal V, Dueker DK. Comparison of optical coherence tomography and ultrasound biomicroscopy for detection of narrow anterior chamber angles. Arch Ophthalmol. 2005; 123: 1053-1059.
17. Wirbelauer C, Karandish A, Häberle H, Pham DT. Noncontact goniometry with optical coherence tomography. Arch Ophthalmol. 2005; 123: 179-185.
18. Cheung CY, Liu S, Weinreb RN, Liu J, Li H. Dynamic analysis of iris configuration with anterior segment optical coherence tomography. Invest Ophthalmol Vis Sci. 2010; 51: 4040-4046.

19. Zheng C, Cheung CY, Narayanaswamy A, Ong SH, Perera SA. Pupil dynamics in Chinese subjects with angle closure. Graefes Arch Clin Exp Ophthalmol. 2012; 250: 1353-1359.

20. Leung CK, Cheung CY, Li H, Dorairaj S, Yiu CK. Dynamic analysis of dark-light changes of the anterior chamber angle with anterior segment OCT. Invest Ophthalmol Vis Sci. 2007; 48: 4116-4122.

21. Chalita MR, Li Y, Smith S, Patil C, Westphal V. High-speed optical coherence tomography of laser iridotomy. Am J Ophthalmol. 2005; 140: 1133-1136.

22. Memarzadeh F, Li Y, Chopra V, Varma R, Francis BA. Anterior segment optical coherence tomography for imaging the anterior chamber after laser peripheral iridotomy. Am J Ophthalmol. 2007; 143: 877-879.

23. Narayanaswamy A, Sakata LM, He MG, Friedman DS, Chan YH. Diagnostic performance of anterior chamber angle measurements for detecting eyes with narrow angles: an anterior segment OCT study. Arch Ophthalmol. 2010; 128: 1321-1327.

24. Savini G, Zanini M, Barboni P. Filtering blebs imaging by optical coherence tomography. Clin Experiment Ophthalmol. 2005; 33: 483-489.

25. Mastropasqua R, Fasanella V, Agnifili L, Curcio C, Ciancaglini M, et al. Anterior segment optical coherence tomography imaging of conjunctival filtering blebs after glaucoma surgery. BioMed research international. 2014.

26. Konstantinidis A, Panos GD, Triantafylla M, Labiris G, Tsaragli E. Imaging of filtering blebs after implantation of the Ex-PRESS shunt with the use of the Visante optical coherence tomography. Int J Ophthalmol. 2015; 8: 492-495.

27. Inoue T, Matsumura R, Kuroda U, Nakashima K, Kawaji T, et al. Precise identification of filtration openings on the scleral flap by three-dimensional anterior segment optical coherence tomography. Investigative ophthalmology & visual science. 2012; 53: 8288-8294.

28. Kojima S, Inoue T, Nakashima K, Fukushima A, Tanihara H. Filtering blebs using 3-dimensional anterior-segment optical coherence tomography: a prospective investigation. JAMA Ophthalmol. 2015; 133: 148-156.

29. Nolan WP, See JL, Chew PT, Friedman DS, Smith SD. Detection of primary angle closure using anterior segment optical coherence tomography in Asian eyes. Ophthalmology. 2007; 114: 33-39.

30. Sakata LM, Lavanya R, Friedman DS, Aung HT, Gao H. Comparison of gonioscopy and anterior segment ocular coherence tomography in detecting angle closure in different quadrants of the anterior chamber angle. Ophthalmology. 2008; 115: 769-774.

31. Pekmezci M, Porco TC, Lin SC. Anterior segment optical coherence tomography as a screening tool for the assessment of the anterior segment angle. Ophthalmic surgery, lasers & imaging : the official journal of the International Society for Imaging in the Eye. 2009; 40: 389-398.

32. Lavanya R, Foster PJ, Sakata LM, Friedman DS, Kashiwagi K. Screening for narrow angles in the singapore population: evaluation of new noncontact screening methods. Ophthalmology. 2008; 115: 1720-1727, 1727.

33. Sakata LM, Lavanya R, Friedman DS, Aung HT, Seah SK. Assessment of the scleral spur in anterior segment optical coherence tomography images. Arch Ophthalmol. 2008; 126: 181-185.

34. Alencar LM, Medeiros FA. The role of standard automated perimetry and newer functional methods for glaucoma diagnosis and follow-up. Indian J Ophthalmol. 2011; 59: 53-58.

35. Tanna AP, Bandi JR, Budenz DL, Feuer WJ, Feldman RM. Interobserver agreement and intraobserver reproducibility of the subjective determination of glaucomatous visual field progression. Ophthalmology. 2011; 118: 60-65.

36. Gillespie BW, Musch DC, Guire KE, Mills RP, Lichter PR, et al. The collaborative initial glaucoma treatment study: baseline visual field and test-retest variability. Investigative ophthalmology & visual science. 2003; 44: 2613-2620.

37. Wang Y, Fawzi AA, Varma R, Sadun AA, Zhang X. Pilot study of optical coherence tomography measurement of retinal blood flow in retinal and optic nerve diseases. Invest Ophthalmol Vis Sci. 2011; 52: 840-845.

38. Kiumehr S, Park SC, Syril D, Teng CC, Tello C. In vivo evaluation of focal lamina cribrosa defects in glaucoma. Arch Ophthalmol. 2012; 130: 552-559.

39. Wang X, Jia Y, Spain R, Potsaid B, Liu JJ. Optical coherence tomography angiography of optic nerve head and parafovea in multiple sclerosis. Br J Ophthalmol. 2014; 98: 1368-1373.

40. Jia Y, Morrison JC, Tokayer J, Tan O, Lombardi L. Quantitative OCT angiography of optic nerve head blood flow. Biomed Opt Express. 2012; 3: 3127-3137.

41. Chen TC. Spectral domain optical coherence tomography in glaucoma: qualitative and quantitative analysis of the optic nerve head and retinal nerve fiber layer (an AOS thesis). Transactions of the American Ophthalmological Society. 2009; 107: 254-281.

42. Kass MA, Heuer DK, Higginbotham EJ, Johnson CA, Keltner JL, et al. The Ocular Hypertension Treatment Study: a randomized trial determines that topical ocular hypotensive medication delays or prevents the onset of primary open-angle glaucoma. Arch Ophthalmol. 2002; 120: 701-713.

43. Miglior S, Zeyen T, Pfeiffer N, Cunha-Vaz J, Torri V. Results of the European Glaucoma Prevention Study. Ophthalmology. 2005; 112: 366-375.

44. Hood DC, Kardon RH. A framework for comparing structural and functional measures of glaucomatous damage. Prog Retin Eye Res. 2007; 26: 688-710.

45. Medeiros FA, Alencar LM, Zangwill LM, Sample PA, Weinreb RN. The Relationship between intraocular pressure and progressive retinal nerve fiber layer loss in glaucoma. Ophthalmology. 2009; 116: 1125-1133.

46. Miki A, Medeiros FA, Weinreb RN, Jain S, He F. Rates of retinal nerve fiber layer thinning in glaucoma suspect eyes. Ophthalmology. 2014; 121: 1350-1358.

47. Hood DC, Fortune B, Mavrommatis MA, Reynaud J, Ramachandran R. Details of Glaucomatous Damage Are Better Seen on OCT En Face Images Than on OCT Retinal Nerve Fiber Layer Thickness Maps. Invest Ophthalmol Vis Sci. 2015; 56: 6208-6216.

48. Ng DS, Gupta P, Tham YC, Peck CF, Wong TY. Repeatability of Perimacular Ganglion Cell Complex Analysis with Spectral-Domain Optical Coherence Tomography. J Ophthalmol. 2015; 2015: 605940.

49. Oli A, Joshi D. Can ganglion cell complex assessment on cirrus HD OCT aid in detection of early glaucoma? Saudi J Ophthalmol. 2015; 29: 201-204.

50. Hayashi K, Araie M, Konno S, Tomidokoro A. Correlation of Macular Ganglion Cell Complex Thickness With Frequency-doubling Technology Perimetry in Open-angle Glaucoma With Hemifield Defects. J Glaucoma. 2015.

51. Park SC, Hsu AT, Su D, Simonson JL, Al-Jumayli M. Factors associated with focal lamina cribrosa defects in glaucoma. Invest Ophthalmol Vis Sci. 2013; 54: 8401-8407.

52. Faridi OS, Park SC, Kabadi R, Su D, De Moraes CG. Effect of focal lamina cribrosa defect on glaucomatous visual field progression. Ophthalmology. 2014; 121: 1524-1530.

53. You JY, Park SC, Su D, Teng CC, Liebmann JM. Focal lamina cribrosa defects associated with glaucomatous rim thinning and acquired pits. JAMA Ophthalmol. 2013; 131: 314-320.

54. Furlanetto RL, Park SC, Damle UJ, Sieminski SF, Kung Y. Posterior displacement of the lamina cribrosa in glaucoma: in vivo interindividual and intereye comparisons. Invest Ophthalmol Vis Sci. 2013; 54: 4836-4842.

55. Lee EJ, Kim TW, Weinreb RN. Reversal of lamina cribrosa displacement and thickness after trabeculectomy in glaucoma. Ophthalmology. 2012; 119: 1359-1366.

56. Lee EJ, Kim TW, Weinreb RN, Kim H. Reversal of lamina cribrosa displacement after intraocular pressure reduction in open-angle glaucoma. Ophthalmology. 2013; 120: 553-559.

57. Strouthidis NG, Fortune B, Yang H, Sigal IA, Burgoyne CF. Longitudinal change detected by spectral domain optical coherence tomography in the optic nerve head and peripapillary retina in experimental glaucoma. Investigative ophthalmology & visual science. 2011; 52: 1206-1219.

58. Park SC, Brumm J, Furlanetto RL, Netto C, Liu Y. Lamina cribrosa depth in different stages of glaucoma. Invest Ophthalmol Vis Sci. 2015; 56: 2059-2064.

59. Francois J, Neetens A. Vascularity of the eye and the optic nerve in glaucoma. Arch Ophthalmol. 1964; 71: 219-225.

60. Kubota T, Jonas JB, Naumann GO. Decreased choroidal thickness in eyes with secondary angle closure glaucoma. An aetiological factor for deep retinal changes in glaucoma? Br J Ophthalmol. 1993; 77: 430-432.

61. Yin ZQ, Vaegan, Millar TJ, Beaumont P, Sarks S. Widespread choroidal insufficiency in primary open-angle glaucoma. J Glaucoma. 1997; 6: 23-32.

62. Spaide RF, Koizumi H, Pozzoni MC. Enhanced depth imaging spectral-domain optical coherence tomography. Am J Ophthalmol. 2008; 146: 496-500.

63. Zhang Z, Yu M, Wang F, Dai Y, Wu Z. Choroidal Thickness and Open-Angle Glaucoma: A Meta-Analysis and Systematic Review. J Glaucoma. 2015.

64. Jonas JB, Steinmetz P, Forster TM, Schlichtenbrede FC, Harder BC. Choroidal Thickness in Open-angle Glaucoma. J Glaucoma. 2015; 24: 619-623.

65. Wang W, Zhang X. Choroidal thickness and primary open-angle glaucoma: a cross-sectional study and meta-analysis. Invest Ophthalmol Vis Sci. 2014; 55: 6007-6014.

66. Maul EA, Friedman DS, Chang DS, Boland MV, Ramulu PY. Choroidal thickness measured by spectral domain optical coherence tomography: factors affecting thickness in glaucoma patients. Ophthalmology. 2011; 118: 1571-1579.

67. Margolis R, Spaide RF. A pilot study of enhanced depth imaging optical coherence tomography of the choroid in normal eyes. Am J Ophthalmol. 2009; 147: 811-815.

68. Pellegrini M, Shields CL, Arepalli S, Shields JA. Choroidal melanocytosis evaluation with enhanced depth imaging optical coherence tomography. Ophthalmology. 2014; 121: 257-261.

69. Flammer J, Orgül S, Costa VP, Orzalesi N, Krieglstein GK. The impact of ocular blood flow in glaucoma. Prog Retin Eye Res. 2002; 21: 359-393.

70. Tobe LA, Harris A, Hussain RM2, Eckert G, Huck A. The role of retrobulbar and retinal circulation on optic nerve head and retinal nerve fibre layer structure in patients with open-angle glaucoma over an 18-month period. Br J Ophthalmol. 2015; 99: 609-612.

71. Jia Y, Wei E, Wang X, Zhang X, Morrison JC. Optical coherence tomography angiography of optic disc perfusion in glaucoma. Ophthalmology. 2014; 121: 1322-1332.

72. Harris A, Rechtman E, Siesky B, Jonescu-Cuypers C, McCranor L. The role of optic nerve blood flow in the pathogenesis of glaucoma. Ophthalmol Clin North Am. 2005; 18: 345-353, v.

73. Wong TY, Mitchell P. The eye in hypertension. Lancet. 2007; 369: 425-435.

74. Hitchings RA, Spaeth GL. Fluorescein angiography in chronic simple and low-tension glaucoma. Br J Ophthalmol. 1977; 61: 126-132.

75. Schwartz B, Rieser JC, Fishbein SL. Fluorescein angiographic defects of the optic disc in glaucoma. Arch Ophthalmol. 1977; 95: 1961-1974.

76. Talusan E, Schwartz B. Specificity of fluorescein angiographic defects of the optic disc in glaucoma. Arch Ophthalmol. 1977; 95: 2166-2175.

77. Huber K, Plange N, Remky A, Arend O. Comparison of colour Doppler imaging and retinal scanning laser fluorescein angiography in healthy volunteers and normal pressure glaucoma patients. Acta ophthalmologica Scandinavica. 2004; 82: 426-431.

78. Arend O, Plange N, Sponsel WE, Remky A. Pathogenetic aspects of the glaucomatous optic neuropathy: fluorescein angiographic findings in patients with primary open angle glaucoma. Brain Res Bull. 2004; 62: 517-524.

79. Hamard P, Hamard H, Dufaux J, Quesnot S. Optic nerve head blood flow using a laser Doppler velocimeter and haemorheology in primary open angle glaucoma and normal pressure glaucoma. Br J Ophthalmol. 1994; 78: 449-453.

80. Piltz-seymour JR, Grunwald JE, Hariprasad SM, Dupont J. Optic nerve blood flow is diminished in eyes of primary open-angle glaucoma suspects. Am J Ophthalmol. 2001; 132: 63-69.

81. Michelson G, Langhans MJ, Harazny J, Dichtl A. Visual field defect and perfusion of the juxtapapillary retina and the neuroretinal rim area in primary open-angle glaucoma. Graefes Arch Clin Exp Ophthalmol. 1998; 236: 80-85.

82. Hafez AS, Bizzarro RL, Lesk MR. Evaluation of optic nerve head and peripapillary retinal blood flow in glaucoma patients, ocular hypertensives, and normal subjects. Am J Ophthalmol. 2003; 136: 1022-1031.

83. Michelson G, Langhans MJ, Harazny J, Dichtl A. Visual field defect and perfusion of the juxtapapillary retina and the neuroretinal rim area in primary open-angle glaucoma. Graefe's archive for clinical and experimental ophthalmology = Albrecht von Graefes Archiv fur klinische und experimentelle Ophthalmologie. 1998; 236: 80-85.

84. Aizawa N, Kunikata H, Shiga Y, Yokoyama Y, Omodaka K. Correlation between structure/function and optic disc microcirculation in myopic glaucoma, measured with laser speckle flowgraphy. BMC Ophthalmol. 2014; 14: 113.

85. Yokoyama Y, Aizawa N, Chiba N, Omodaka K, Nakamura M, et al. Significant correlations between optic nerve head microcirculation and visual field defects and nerve fiber layer loss in glaucoma patients with myopic glaucomatous disk. Clinical ophthalmology. 2011l; 5: 1721-1727.

86. Aizawa N, Yokoyama Y, Chiba N, Omodaka K, Yasuda M, et al. Reproducibility of retinal circulation measurements obtained using laser speckle flowgraphy-NAVI in patients with glaucoma. Clinical ophthalmology. 2011; 5: 1171-1176.

87. Nicolela MT, Hnik P, Schulzer M, Drance SM. Reproducibility of retinal and optic nerve head blood flow measurements with scanning laser Doppler flowmetry. J Glaucoma. 1997; 6: 157-164.

88. Tan O, Wang Y, Konduru RK, Zhang X, Sadda SR. Doppler optical coherence tomography of retinal circulation. J Vis Exp. 2012; 67: e3524.

89. Hwang JC, Konduru R, Zhang X, Tan O, Francis BA. Relationship among visual field, blood flow, and neural structure measurements in glaucoma. Invest Ophthalmol Vis Sci. 2012; 53: 3020-3026.

90. Sehi M, Goharian I, Konduru R, Tan O, Srinivas S. Retinal blood flow in glaucomatous eyes with single-hemifield damage. Ophthalmology. 2014; 121: 750-758.

91. Tan O, Liu G, Liang L, Gao SS, Pechauer AD. En face Doppler total retinal blood flow measurement with 70 kHz spectral optical coherence tomography. J Biomed Opt. 2015; 20: 066004.

92. Liu L, Jia Y, Takusagawa HL, Pechauer AD, Edmunds B. Optical Coherence Tomography Angiography of the Peripapillary Retina in Glaucoma. JAMA Ophthalmol. 2015; 133: 1045-1052.